

Penguin Huddling inspired Distributed Boundary Movement for Group Survival in Multi-robot Systems using Gaussian Processes

Tamzidul Mina¹ and Byung-Cheol Min²

Abstract—Traditionally, research on mobile robot adaptability to damaging external stimuli has only focused on making individuals capable of surviving on their own, which is often very expensive and lacks robustness. In this paper, we present our *initial* work on an Emperor Penguin huddling-inspired group survival methodology for a multi-robot system exposed to a damaging directional external stimulus. Individuals on the stimuli side are able to relocate to the safest location on the leeward side of the group in turns without any communication requirements or prior knowledge of the group size or shape, for prolonged survival of the group as a whole. A distributed boundary movement method is proposed with Gaussian Processes machine learning that allows individuals to relocate to the robot health-loss-rate global minima around the group boundary only using stimuli measurements. Simulation results validate our proposed methodology of successfully relocating individuals. The robustness of the proposed method was tested under different formation sizes and shapes. In all cases, successful relocation was obtained. As an effect, significant improvement in survivability of the robot group as a whole was obtained.

I. INTRODUCTION

Robots play an important role in exploring the unknown and in some of the harshest environments on Earth [1]. To survive severe damaging environments (strong directional winds, blizzards, dust storms, etc.), individual robots have traditionally required custom-built hardware to survive long-term exposure to extreme external stimuli. For instance, robots built for Antarctic explorations (such as NOMAD [2] and Cool [3]) encounter extreme cold temperatures and strong damaging winds even in the Antarctic summer [4]. In such conditions, electronic components require specially sealed, insulated, aerogel warm-housing [5] [6] for normal operation; lithium batteries despite being a popular choice, suffer severe power loss at temperatures below 0°C [7]. Warm-up routines are often required as well to keep lubricants from stiffening. Such adaptations are expensive and in most cases specific to individuals and environmental conditions. Given the unpredictable nature of such conditions, designing individual robots that can take into account all possible scenarios is not feasible either.

Emperor Penguins in the Antarctic are able to survive one of the harshest environments on Earth (temperatures below -45°C , winds over 100mph [8]) by working as a group.

¹Tamzidul Mina is with the SMART Lab, Department of Computer and Information Technology, Purdue University, and with the School of Mechanical Engineering, Purdue University, West Lafayette, IN 47907, USA tmina@purdue.edu

²Byung-Cheol Min is with the SMART Lab, Department of Computer and Information Technology, Purdue University, West Lafayette, IN 47907, USA minb@purdue.edu



Fig. 1: Penguin huddling in the Antarctic winter showing boundary movements from the windward to the leeward side. Image taken from the *PBS Nature* show.

During Antarctic storms, the penguins huddle together [9] in tight groups. An observation described in [10] suggest that under strong wind conditions, Emperor penguins on the windward side slowly move down the flanks to the leeward side and position themselves behind the huddle. The penguins that are now exposed follow and position themselves behind the ones who moved in previously; the process continues so that everyone gets an equal opportunity to stay protected by being downwind and eventually the center; none are left behind. Fig. 1 shows penguin huddling and boundary movement in the Antarctic winter.

While Emperor penguins have evolved to withstand very low temperatures on their own, they can only survive conditions as severe as Antarctic winters by being in a social group. Individual robots have been traditionally designed the same way, but we ask the question how being in a group can increase robustness in survivability. Similar to how penguins take turns being on the leeward side of the group during storms, robots could take turns settling on the leeward side to minimize damage by physical protection from the group when no shelter is available nearby. In this paper, we propose a distributed boundary movement methodology using Gaussian Processes machine learning with a spectral mixture kernel to relocate individuals from the stimuli side to the health-loss-rate global minima on the leeward side without requiring any communication or prior knowledge of group size or shape when exposed to a damaging directional external stimuli.

II. RELATED WORK

Body heat and the energy saving benefits of penguin huddling and shuffling has been studied in [11]. The dynamic movements in the huddle that allow an equal opportunity for all penguins to be at the center based on temperature changes within the huddle was explained in [9]. Despite

numerous extensive studies, very few theoretical models of the boundary movement in a huddle has been put forward.

A theoretical model focused on the boundary movements of huddling penguins moving from the windward side to the leeward side was first proposed in [12]. Waters *et al.* [13] extended that work by taking into account an inviscid and irrotational wind flow and a temperature profile around the huddle. The huddle was created as a hexagonal grid based on [8] and assumed that the penguins did not displace one another and the penguin with the highest heat loss relocated to the centrally pre-computed best location in the huddle.

Previous work on robots following a boundary using machine learning include a wall-following robot that used linear regression and Support Vector Regression to predict motor commands to determine the direction of motion [14]. Programmable self-assembly of multi-robots was achieved by [15] using Kilobots [16] following the boundary of the group to form complex planar prescribed shapes. A centralized approach of robot relocation in a structured robot formation was previously studied in [17] assuming full communication and state information.

Adaptive behaviors by robots to external stimuli have primarily focused on peripheral stages of sensory perception or on peripheral motor control [18][19]. Conditioned reward-based behavior to adapt to external stimuli using spiking neural networks was proposed by [20].

For our multi-robot system with distributed control and without communication, we build on the huddle modeling work by Waters *et al.* [13]. Since the robots are unaware of the size and shape of the huddle, nor have any information on a suitable safe relocation position, this paper proposes a machine learning approach where robots move along the boundary looking for a favorable position to relocate to, only relying on external stimuli readings and distance to neighbors. Our proposed method combines learning algorithms in artificial intelligence to multi-robot group survival decision making in extreme environments in a distributed manner.

A. Robot group formation and movement dynamics

We consider a scenario where a robot group has been deployed on a long-term mission without any human supervision and encounters a severe external stimuli without any shelter nearby. The huddling behavior of Emperor penguins involve tight packing of individuals for group survival. Therefore, we consider a closed hexagonal lattice formation for our group of robots with no empty spaces within the robot group. We let $r_i^t \in \mathbb{R}^2$ denote the position of the i^{th} robot R_i on a planar surface with respect to a global inertial frame for $i = \{1, 2, \dots, N\}$ at time instant t , with a neighbor detection radius of r_d . For simplicity, we model the robots as point masses with full actuation. The dynamic model of the i^{th} robot can be written as, $\dot{r}_i = v_i$, $\dot{v}_i = u_i$; where v_i and u_i denote the absolute velocity and the control force for the corresponding robot i .

At any given time t , R_i can either be staying in formation ($i \in A$) or moving along the boundary ($i \in B$) where A is defined as the set of robots staying in formation and B

the set of robots moving around the boundary. We assume every robot is equipped with distance sensors and are able to classify neighboring robots within r_d to be in A or B . We model robots in A and B to only interact with robots in their own set. This ensures that boundary moving robots do not displace robots that are currently in formation.

The hexagonal lattice formation with robots in A is maintained using an interaction force f_I derived from an artificial potential F_I previously established in [21] written as,

$$F_I = \begin{cases} \alpha_I (\ln(r_{ij}) + \frac{d_0}{r_{ij}}) & 0 < r_{ij} < d_1 \\ \alpha_I (\ln(r_{d_1}) + \frac{d_0}{d_1}) & r_{ij} \geq d_1 \end{cases} \quad (1)$$

$$f_I = \begin{cases} \nabla_{r_{ij}} F_I & 0 < r_{ij} < d_1 \\ 0 & r_{ij} \geq d_1 \end{cases} \quad (2)$$

where r_{ij} is the distance between robots i and j in A , α_I is a scalar control gain; d_0 and d_1 are scalar constants such that $d_0 < d_1 \leq r_d$. At equilibrium, all robots are grouped together in the hexagonal lattice formation. The hexagonal lattice formation is locally stable in the sense of Lyapunov because by design, the equilibrium is a global minimum of the total artificial potential [21]. Robots in B also interact with other members of B exclusively using Eq. (1)-(2) to prevent collision.

We define an artificial potential F_d and the attractive force f_d for the *tangential* boundary movement of robot R_i , $i \in B$ around its closest neighbor R_j , $j \in A$ by,

$$F_d = \frac{1}{2} \alpha_d r_{ij}^2 \quad f_d = \nabla F_d \quad (3)$$

where α_d is a scalar gain constant, $r_{ij} \leq r_d$ is the distance between R_i and R_j . We denote f_t as the tangential force vector derived with magnitude equal to $\|f_d\|$ and direction $\theta_t = \theta_d + \eta \frac{\pi}{2}$, where θ_d denotes the direction of f_d and $\eta \in \{1, -1\}$ depending on the direction of movement. Therefore, the control input can be written as,

$$u_i = \begin{cases} -\sum_{j \neq i, j \neq m}^N f_t(r_{ij}) & i, j \in A, m \in B \\ -f_t(r_{ij}) & i \in B, j \in A. \end{cases} \quad (4)$$

We constraint each robot with a maximum velocity v_m .

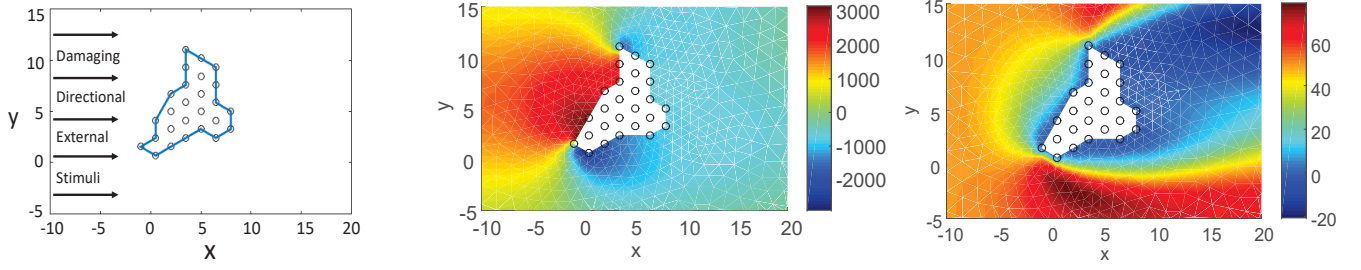
III. PROPOSED SOLUTION

A. Modeling Damaging Directional External Stimuli and Robot Health Loss

For a multi-robot group on a planar surface modeled as a hexagonal lattice formation, we assume a damaging external stimuli from the left, detrimental to the set of exposed robots. The setup is illustrated in Fig. 2a. To maintain generality of a damaging directional external stimuli, we set the following requirements:

- A direct damaging *force* on the stimuli side.
- Stimuli affects flank members exposed to the outside.
- Direct protection is only available on the leeward side.

We model such a damaging external stimuli as a directional, viscous and incompressible fluid flow with an inlet on the $x = -10$ line, flow directed towards x^+ with inlet



(a) A hexagonal lattice formation of $N=26$ robots. A damaging directional external stimuli is present along the x^+ direction. (b) Pressure/Density ($units^4/t^2$) distribution from modeling the damaging directional external stimuli as a fluid flow. (c) x -velocity ($units/t$) distribution from modeling the damaging directional external stimuli as a fluid flow.

Fig. 2: Damaging directional external stimuli as a viscous incompressible flow around the robot formation.

velocity, $v_x = v_f$ around our robot group. Fig. 2b-2c show the *pressure/density* distribution and v_x distribution of the fluid around the robot group respectively. We assume high *pressure/density* zones and high v_x zones as damaging elements to an exposed robot in the group. The modeled fluid flow fulfills our set requirements for a damaging directional external stimuli as follows:

- Creates a high pressure zone on the stimuli side (*analogous to a direct damaging force*).
- Flanks experience high fluid velocity with variations in pressure (*damaging for exposed flank robots*).
- A low absolute pressure zone with low fluid velocity on the leeward side (*protected zone*).

The illustrated fluid flow was simulated in the MATLAB QuickerSim toolbox with viscous coefficient $\nu = 10$. We assume that robots have negligible spacing in between such that the robot group may be considered a solid non-deformable planar object. Thus, the fluid flow model may be simplified as a flow around a single solid object.

At time t , R_i measures the external stimuli at its location r_i to determine its rate of health loss written as,

$$L_i^t = \begin{cases} \frac{\beta_P |P_i^t| + \beta_V V_i^t}{n_i^t} & \text{if } n_i^t < 6 \\ 0 & \text{else} \end{cases} \quad (5)$$

where β_P and β_V are scaling constants, P_i^t and V_i^t are measured pressure and fluid velocity and n_i^t is the number of neighbors detected within r_d .

R_i , $i \in A$ breaks off the formation if $L_i^t > L_{t,threshold}$, such that R_i for $A \leftarrow A \setminus \{i\}$, $B \leftarrow B \cup \{i\}$ starts moving along the boundary with η determined as away from the direction of the damaging external stimuli.

B. Boundary Movement using Gaussian Processes estimated Global minima

Once movement is initialized for R_i , $i \in B$ the time is recorded as t^i . R_i , $i \in B$ continues to move along the boundary unaware of the size and shape of the robot group, without moving backwards or displacing neighboring robots, measuring fluid pressure P_i^t , fluid velocity V_i^t at coordinates $r_i^t = (x_i^t, y_i^t)$ at every time instant $t \geq t^i$. Without any communication it is unable to determine its safest relocation position from the group where absolute pressure and fluid velocity are

lowest suggesting a minimal L_i position from the external stimuli. We denote the current time as t_c .

Gaussian Processes (GP) are a powerful regression technique which provide Bayesian non-parametric smoothing and interpolation with a set of basis functions. We define a distribution over functions $f(x)$,

$$\begin{aligned} f(x) &\sim \mathcal{GP}(m(x), k(x, x')) \\ m(x) &= \mathbb{E}[f(x)] \\ k(x, x') &= \text{cov}(f(x), f(x')) \end{aligned} \quad (6)$$

where $x \in \mathbb{R}^S$ is an arbitrary input variable over space S , $m(x)$ is the mean and $k(x, x')$ is the covariance function respectively.

The properties of the likely functions under a GP are controlled by the positive definite covariance function. The choice of the kernel affects performance significantly on a given task. A commonly used kernel function is the *squared exponential* (SE) kernel (7) where the only covariance structure learned from training data is the length scale l ,

$$k_{SE}(x, x') = \exp(-0.5 \|x - x'\|^2 / l^2). \quad (7)$$

However, by using a mixture of Gaussians that have non-zero means, a much wider range of spectral densities can be obtained [22]. Therefore, for better performance we use the spectral mixture (SM) kernel,

$$k_{SM}(\tau) = \sum_{q=1}^Q w_q \prod_{s=1}^S \exp\{-2\pi^2 \tau_s^2 v_q^{(s)}\} \cos 2\pi \tau_s \mu_q^{(s)} \quad (8)$$

where w_q are weights that specify the relative contribution of each mixture component, Q is the number of Gaussians on \mathbb{R}^S with the q^{th} component having mean $\mu_q = (\mu_q(1), \dots, \mu_q(S))$ and covariance matrix $M_q = \text{diag}(v_q(1), \dots, v_q(S))$ and τ_s is the s^{th} component of the S dimensional vector $\tau = (x - x')$.

The advantage of GP over other learning approaches is that it provides well defined confidence intervals important to assess the predicted model. Therefore, we propose GP machine learning at time intervals of t_{int} for R_i , $i \in B$ to determine pressure and velocity models $f_i^P(t)$ and $f_i^V(t)$ as trends in P_i^t and V_i^t measurements collected as training data between $t^i \leq t \leq t_c$ respectively, and extrapolate the models to predict if a better relocation position is available ahead up

TABLE I: Simulation parameters

Simulation scenario	Conditions for robot relocation
S1	GP estimated global minima
S2	Local minima with $L_i^c < L_i^t$
S3 (control)	Robots do not relocate

TABLE II: Simulation parameters

Parameter	Value	Parameter	Value
d_0	$\sqrt{3}$ units	β_P/β_V	2.05
d_1	$d_0\sqrt{3}$ units	α_l	4
λ_1/λ_2	2.05	α_d	8
t_{tol}	$2ts$	v_m	0.25 units/ts
t_{int}	$5ts$ for $(t_c - t^i) > 30ts$	r_d	d_1
$L_{threshold}$	0.01		

to time t_{extrap} . We define a cost function $L_i^c(t)$ using weighted $f_i^P(t)$ and $f_i^V(t)$ components and determine a *global minima* corresponding to the safest location in the group at $t = t_{min}$. The cost function L_i^c is defined as,

$$L_i^c(t) = \lambda_1 |f_i^P(t)| + \lambda_2 f_i^V(t) \quad (9)$$

$$t_{min} = \arg \min_i L_i^c \quad (10)$$

where λ_1 and λ_2 are weights of each component. The *global minima* is determined by a simple *exhaustive search*.

After every GP iteration at time interval t_{int} , the determined t_{min} is compared to t_c to assess if $R_i, i \in B$ should settle or continue to move. If $t_c - t_{tol} \leq t_{min} \leq t_c + t_{tol}$, where t_{tol} is a defined tolerance constant, implying that t_{min} has been found within a certain tolerance of the current iteration time t_c , then the best location is in the immediate vicinity of r_i^c and R_i settles at the current location $B \leftarrow B \setminus \{i\}, A \leftarrow A \cup \{i\}$. If not, $R_i, i \in B$ continues to move along the boundary in the same direction for $t_{min} > t_c + t_{tol}$. We ensure $t_{min} \geq t_c - t_{tol}$ is always true such that $R_i, i \in B$ does not have to move backwards by setting a small enough t_{int} . With more training data after every iteration, the predicted models improve over time providing better estimations of the global minima.

IV. VALIDATION

A. Simulation Setup

To validate our proposed method, we show that $R_i, i \in \{1, 2, \dots, N\}$ on the exposed side of the group is successfully able to move from the stimuli-side to the leeward side health-loss-rate global minima of the group, using external stimuli measurements only, without any communication requirements or prior knowledge of the group size or shape.

The validation process is set up with three scenarios to establish the need and effectiveness of our proposed GP global estimation method for distributed robot relocation as presented in Table I. We compare S1 and S2 to show the importance of using a relocation by health-loss-rate global minima approach in comparison to local minima; the use of a learning algorithm is also justified. We compare S1 with S3 to show the extent of improved survivability of individual robots and the group as a whole with the proposed method, in comparison to a control group where robots do not relocate or seek safety. We consider a group of $N = 26$

robots in a closed hexagonal lattice formation on a plane as previously shown in Fig. 2a. The group is exposed to a damaging directional external stimuli modeled as a viscous incompressible fluid flow from the left with $v_f = 1$ units/ t and $\nu = 10$ as shown in Fig. 2b - 2c. We assume the following:

- Robots do not communicate with each other.
- Robots do not displace each other.
- Robots can measure distance to neighbors within r_d .
- Robots can measure external stimuli.
- All robots are identical in shape and size.

For demonstration purposes, we track and present the progress of five randomly picked robots from the stimuli side at t_0 denoted as $R_i, i \in G_{26}$ where $G_{26} = \{12, 15, 23, 24, 25\}$. For all scenarios, we initialize the simulation at time t_0 with sampling time $\partial t = 0.1$ and time step unit written as (ts). At $t_0, \forall R_i, i \in A$. At every time instant t , R_i determines its L_i^t using (5). For comparison between the scenarios, we denote the final health-loss-rate for $R_i, i \in G_{26}$ when settling under S1 as $(L_i^t)_{S1}$ and S2 as $(L_i^t)_{S2}$. The simulation parameters used are exaggerated for brevity and are listed in Table II. r_d is chosen to be the minimum distance to possible immediate neighbors to show the effectiveness of the proposed algorithm even with limited sensing. The proposed concept of relocating individuals to the leeward side is a continuous process in the group; for presentation and analysis purposes the simulation is stopped at $t = 50$.

B. Relocation using S1 vs. S2

1) *S1*: Fig. 3 shows the progress of the boundary movement of $R_i, i \in G_{26}$ along with the fluid pressure and velocity distribution around the robot group with changing boundary at specific time intervals. Fig. 4 tracks the corresponding L_i^t for robots $R_i, i \in G_{26}$ following their boundary movements.

At t_0 , R_{15}, R_{23}, R_{24} and R_{25} are directly exposed to the external stimuli and start to move along the boundary as shown at time $t = 0.2$. At $t = 0.6$, R_{12} becomes exposed as R_{15} and R_{25} moved away; therefore, R_{12} starts to move along the boundary as well, as shown at time $t = 4.1$. R_{24} was successfully able to determine its global minima on the leeward side at $t = 13.1$, followed by R_{23} at $t = 14.7$. R_{25} reached a minima close to zero at $t = 13.2$ but continued to move based on its estimation of a global minima being further ahead. R_{25} finally settled at $t = 29.7$. R_{15} and R_{12} settled around the same time at $t = 29.5$ and $t = 29.6$.

L_{24}^t reached zero after $t > 12$ as it was surrounded on all sides by neighbors; $L_{12}^t, L_{15}^t, L_{23}^t$ and L_{25}^t get very close to zero since the corresponding robots stay on the boundary of the robot group even at $t = 41.4$. L_{avg}^t plots the average health loss rate of the five tracked robots in Fig 4.

While moving around the flanks and extrema of the group boundary, all robots experienced a sudden increase in L_i^t . In this region, v_x is at its peak along with very low pressure. Since L_i^t considers the absolute value of the pressure component, the robots experienced the highest health loss rate here modeled by (5) as opposed to the stimuli-side where v_x is low with very high pressure. Regardless, Gaussian Processes

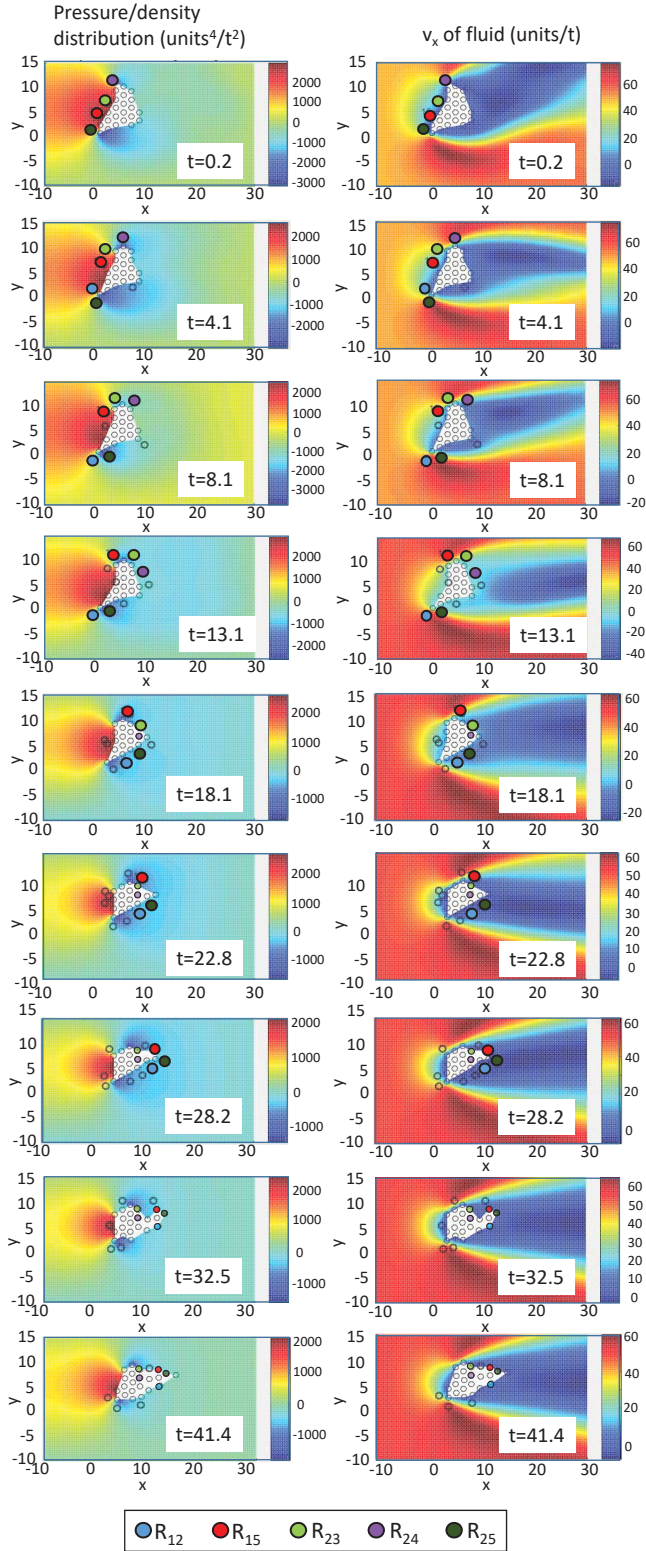


Fig. 3: Simulation time-lapse for $N = 26$ in S1, showing the progress of five randomly picked robots (R_{12} , R_{15} , R_{23} , R_{24} , and R_{25}) in G_{26} exposed to a damaging directional stimuli along the x^+ direction. The robots successfully move along the boundary from the damaging stimuli side to the leeward side of the group and settle at the health-loss-rate global minima determined by the proposed GP estimated global minima methodology.

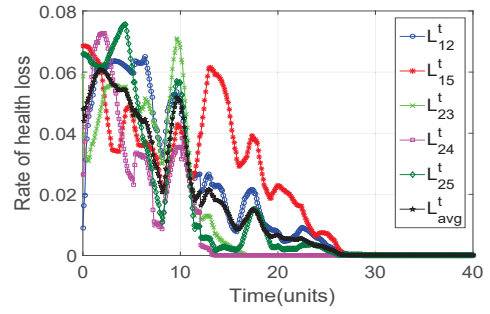


Fig. 4: L_i^t for $i \in G_{26}$ in S1 decreases with time as the robots move from the damaging stimuli side to the leeward side using the proposed GP estimated global minima methodology.

estimation was able to cope with such extreme fluctuations to determine the overall trend in the measurements; the global minima in terms of health loss rate was determined to be further ahead for each robot. No communication was necessary at any time between the robots for relocation.

The relocation process continued for other robots as well and over time as more and more robots successfully relocated to the leeward side, an aerodynamic group boundary was obtained as shown at $t = 41.4$. The protruding flanks of the initial robot group boundary gave away creating a streamlined shape and the initial high pressure zone on the stimuli side shrank considerably over time.

2) S2: The simulation was repeated with the same robot group setup of $N = 26$ and damaging external stimuli model with robots measuring P_i^t and V_i^t at every time instant and relocating to L_i^t local minima. As R_i moved with time, the change in the calculated L_i^t was checked continuously for a local minima. Upon determining the local minima at time t_{min} , if $t_c - t_{tol} \leq t_{min} \leq t_c + t_{tol}$, R_i settled at t_c if $L_i^c < L_i^t$.

The simulation progression of S2 at time instants $t = 22.8$ and $t = 44.4$ is shown in Fig. 5 and the corresponding L_i^t , $i \in G_{26}$ is plotted in Fig. 6. Comparing the progress of S2 with S1 at $t = 22.8$ and $t = 41.4$ in Fig. 5 and Fig. 3 respectively, we make the following observations:

- R_{12} , R_{15} , R_{24} and R_{25} settled at boundary extrema in the local minima case with final $(L_i^t)_{S2} > (L_i^t)_{S1}$ at the end of $t = 41.4$.
- R_{23} was unable to follow the same path as before because of frequently changing group boundary in the local minima case and was still moving after $t = 41.4$.

In the local minima case, individual robots moved short distances to a local minima and settled for short periods of time before moving again. With this method of moving, individuals are constantly moving and settling and may eventually reach a rate of health loss global minima at a certain time and position around the fast changing boundary, but it is not guaranteed. The local minima method was chaotic in comparison and did not allow individuals an equal opportunity to reach the best available position around the group boundary for survival. The global minima methodology also created an aerodynamic group boundary over time as opposed to the local minima methodology where the flanks

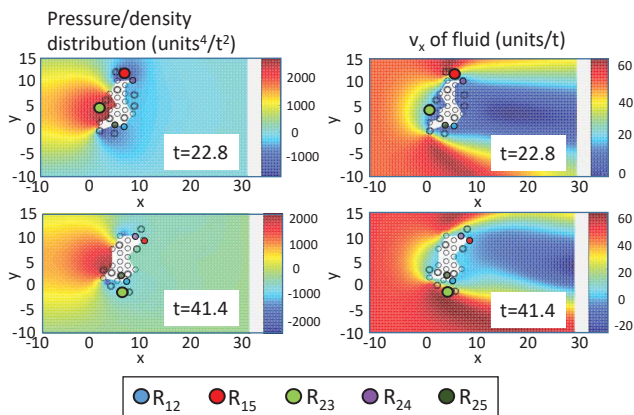


Fig. 5: Simulation time instances for $N = 26$ in S2, showing the progress of five randomly picked robots in G_{26} exposed to a damaging directional stimuli along the x^+ direction. The robots settle along the group flank boundary using the local minima methodology.

expanded as seen at time $t = 41.4$ in Fig 5. Such observations prove that the proposed Gaussian Processes estimated health-loss-rate global minima method is essential for group survival of individuals in the long run.

C. Scalability of proposed method

To verify that the conclusions from S1 hold true over a range of N , the simulation was repeated for $N = 35, 70$ and 107 with arbitrary formation shapes against the same modeled fluid flow as external stimuli. For each N case, five randomly picked robots R_i on the stimuli side of the group were tracked; $i \in G_{35}$ for $N = 35$, $i \in G_{70}$ for $N = 70$ and $i \in G_{107}$ for $N = 107$ where $G_{35} = \{11, 14, 25, 26, 27\}$, $G_{70} = \{52, 53, 58, 61, 69\}$ and $G_{107} = \{21, 32, 74, 97, 103\}$, respectively. Their health loss rate L_i^t with time corresponding to movement around the boundary is shown in Fig. 7a-7c. The simulations were allowed to run up to $t = 50$.

In each case, all tracked robots were able to successfully move from the stimuli side to the estimated best location on the leeward side. For $N = 35$ and $N = 70$, all tracked robots were able to move at $t = t_0$. For $N = 107$, R_{21} regardless of having $L_{21}^t > L_{threshold}$ at $t = t_0$ was unable to move without displacing a neighbor. The sudden increase in L_{21}^t between $9 < t < 12$ is as a result of its neighbors moving away for relocation leaving R_{21} with a higher L_{21}^t and able to move. We denote the average time required for convergence of L_{avg}^t to the health-loss-rate global minima as t_{min}^{avg} , t_{min}^{avg} for $N = 26$ is significantly smaller than t_{min}^{avg} for $N = 107$ because of the large difference in group size. However, t_{min}^{avg} for $N = 70$ is greater than t_{min}^{avg} for $N = 107$. This is because the initial shape of the $N = 70$ robot group had larger protruding flanks than $N = 107$. As a result, robots on the stimuli side for $N = 70$ had to travel longer distances in comparison to reach the health loss global minima on the leeward side. This observation suggested that t_{min}^{avg} for different N cases has a strong correlation with the size and shape of the robot group. Regardless, the scalability of the proposed GP estimated global-minima method in this paper was established without

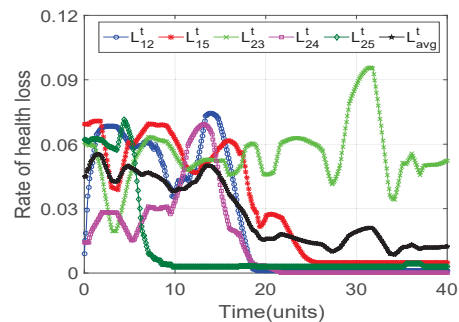


Fig. 6: L_i^t for $i \in G_{26}$ in S2 decreases with time for *some* individuals as the robots move along the boundary to relocate using the local minima methodology.

any effects on the outcome due to group size or shape.

D. Effectiveness of the proposed method: S1 vs. S3

The effectiveness of the proposed method is established by comparing the average robot health of the five randomly picked robots in the same robot groups in S1 with control scenario S3, when encountering the same modeled damaging directional external stimuli. For all the simulation cases of $N = 26, 35, 70$ and 107 in both scenarios, each of the five tracked robots started with full health. We denote the robot health at every time step when allowed to move as H_i^t and when not allowed to move as ${}_nH_i^t$. At every time step for both cases, H_i^t and ${}_nH_i^t$ deteriorate by the corresponding L_i^t for each robot. The average robot health for the five tracked robots for each N case in S1 and S3 are denoted as H_{avgN}^t and ${}_nH_{avgN}^t$ respectively. All simulations for both scenarios were allowed to run up to $t = 50$. The results of the comparison are shown in Fig. 8.

In S3, ${}_nH_{avgN}^t$ for all cases of N deteriorated linearly with time depending on individual L_i^t measurements. For S1, H_{avgN}^t leveled out over time with 18.42%, 16.67%, 35.83% and 29.41% more health at $t = 50$, for $N = 26, 35, 70$ and 107 respectively.

As more robots relocate behind the initially moved robots in S1 in a continuous process, every robot in the group gets an opportunity to reduce their rate of health loss by relocating to the safest available position behind the group. As a result, the whole group is able to survive together for a longer period of time in the field.

A video of the simulations is available for reference at <https://youtu.be/aEujdGRx2HY>.

V. CONCLUSIONS & FUTURE WORK

In this paper, an Emperor Penguin huddling-inspired multi-robot group survival methodology of surviving a directional damaging external stimuli is proposed. A distributed boundary movement control method is presented that allow robots to move from the stimuli-side to the safest available position on the leeward side without requiring any communication with each other or prior knowledge of group size or shape. Gaussian Processes machine learning with SM kernel is used to determine the best relocating position for the moving robot based on only stimuli measurements.

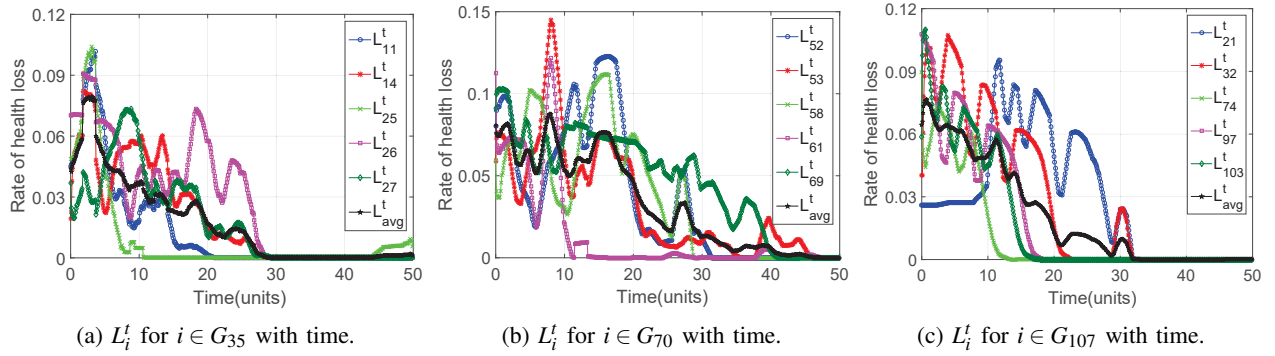


Fig. 7: L_i^t for the tracked robots in each of the $N = 35$, $N = 70$ and $N = 107$ cases for S1 decreases with time as the robots move from the damaging stimuli side to the leeward side using the proposed GP estimated global minima method.

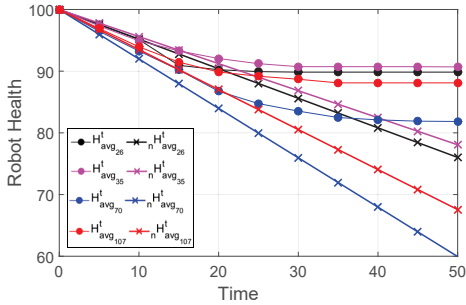


Fig. 8: The average robot health of tracked robots in all N cases was consistently better for S1 (proposed GP estimated global minima method) than control scenario S3 over time.

With successful preliminary simulation results, further work studying the effects of changing external stimuli on the robot group, distributed formation change to minimize stimuli damage and experimental validation is ongoing.

ACKNOWLEDGMENT

The authors would like to thank Prof. Galen King for his constructive criticism on the presented work and Dr. Ramviyas Parasuraman for his invaluable suggestions on Gaussian Processes.

REFERENCES

- [1] B. Ristic, D. Anglely, B. Moran, and J. L. Palmer, "Autonomous multi-robot search for a hazardous source in a turbulent environment," *Sensors*, vol. 17, no. 4, p. 918, 2017.
- [2] D. S. Apostolopoulos, L. Pedersen, B. N. Shamah, K. Shillcutt, M. D. Wagner, and W. L. Whittaker, "Robotic antarctic meteorite search: Outcomes," in *Robotics and Automation, 2001. Proceedings 2001 ICRA. IEEE International Conference on*, vol. 4. IEEE, 2001, pp. 4174–4179.
- [3] J. H. Lever, A. Streeter, and L. Ray, "Performance of a solar-powered robot for polar instrument networks," in *Robotics and Automation, 2006. ICRA 2006. Proceedings 2006 IEEE International Conference on*. IEEE, 2006, pp. 4252–4257.
- [4] L. Valenziano and G. Dall'Oglio, "Millimetre astronomy from the high antarctic plateau: site testing at dome c," *Publications of the Astronomical Society of Australia*, vol. 16, no. 2, pp. 167–174, 1999.
- [5] L. Ray, A. Price, A. Streeter, D. Denton, and J. H. Lever, "The design of a mobile robot for instrument network deployment in antarctica," in *Robotics and Automation, 2005. ICRA 2005. Proceedings of the 2005 IEEE International Conference on*. IEEE, 2005, pp. 2111–2116.
- [6] B. Ratnakumar, M. Smart, A. Kindler, H. Frank, R. Ewell, and S. Surampudi, "Lithium batteries for aerospace applications: 2003 mars exploration rover," *Journal of power sources*, vol. 119, pp. 906–910, 2003.
- [7] Y. Ji, Y. Zhang, and C.-Y. Wang, "Li-ion cell operation at low temperatures," *Journal of The Electrochemical Society*, vol. 160, no. 4, pp. A636–A649, 2013.
- [8] D. P. Zitterbart, B. Wienecke, J. P. Butler, and B. Fabry, "Coordinated movements prevent jamming in an emperor penguin huddle," *PLoS one*, vol. 6, no. 6, p. e20260, 2011.
- [9] C. Gilbert, G. Robertson, Y. Le Maho, Y. Naito, and A. Ancel, "Huddling behavior in emperor penguins: dynamics of huddling," *Physiology & Behavior*, vol. 88, no. 4, pp. 479–488, 2006.
- [10] Y. Le Maho, "The emperor penguin: A strategy to live and breed in the cold: Morphology, physiology, ecology, and behavior distinguish the polar emperor penguin from other penguin species, particularly from its close relative, the king penguin," *American Scientist*, vol. 65, no. 6, pp. 680–693, 1977.
- [11] C. Gilbert, S. Blanc, Y. Le Maho, and A. Ancel, "Energy saving processes in huddling emperor penguins: from experiments to theory," *Journal of Experimental Biology*, vol. 211, no. 1, pp. 1–8, 2008.
- [12] G. Stead, "Huddling behaviour of emperor penguins," *Master's thesis, University of Sheffield, United Kingdom*, 2003.
- [13] A. Waters, F. Blanchette, and A. D. Kim, "Modeling huddling penguins," *PLoS One*, vol. 7, no. 11, p. e50277, 2012.
- [14] C. D. Hassall, R. Bhargava, T. Trappenberg, and O. E. Krigolson, "A robust wall-following robot that learns by example," in *Dalhousie Computer Science In-House Conference (DCSI)*, 2012.
- [15] M. Rubenstein, A. Cornejo, and R. Nagpal, "Programmable self-assembly in a thousand-robot swarm," *Science*, vol. 345, no. 6198, pp. 795–799, 2014.
- [16] M. Rubenstein, C. Ahler, and R. Nagpal, "Kilobot: A low cost scalable robot system for collective behaviors," in *Robotics and Automation (ICRA), 2012 IEEE International Conference on*. IEEE, 2012, pp. 3293–3298.
- [17] T. Mina and B.-C. Min, "Penguin huddling-inspired energy sharing and formation movement in multi-robot systems," in *2018 IEEE International Symposium on Safety, Security, and Rescue Robotics (SSRR)*. IEEE, 2018, pp. 1–8.
- [18] B. Mitchinson, M. Pearson, A. G. Pipe, and T. J. Prescott, "Biomimetic robots as scientific models: a view from the whisker tip," *Neuromorphic and Brain-Based Robots*, pp. 23–57, 2011.
- [19] S. Soltic and N. Kasabov, "A biologically inspired evolving spiking neural model with rank-order population coding and a taste recognition system case study," *System and Circuit Design for Biologically-Inspired Intelligent Learning*, p. 136, 2011.
- [20] L. I. Helgadottir, J. Haenicke, T. Landgraf, R. Rojas, and M. P. Nawrot, "Conditioned behavior in a robot controlled by a spiking neural network," in *Neural Engineering (NER), 2013 6th International IEEE/EMBS Conference on*. IEEE, 2013, pp. 891–894.
- [21] N. E. Leonard and E. Fiorelli, "Virtual leaders, artificial potentials and coordinated control of groups," in *Decision and Control, 2001. Proceedings of the 40th IEEE Conference on*, vol. 3. IEEE, 2001, pp. 2968–2973.
- [22] A. Wilson and R. Adams, "Gaussian process kernels for pattern discovery and extrapolation," in *International Conference on Machine Learning*, 2013, pp. 1067–1075.